Steel and Composite Structures, *Vol. 24, No. 1 (2017) 23-35*
DOI: https://doi.org/10.12989/scs.2017.24.1.023

Push-out test on the one end welded corrugated-strip connectors in steel-concrete-steel sandwich structure

Mehdi Yousefi [a] and Mansour Ghalehnovi [*]

Civil Engineering Department, Faculty of Engineering, Ferdowsi University of Mashhad, Mashhad, Iran

(*Received October 25, 2016, Revised February 17, 2017, Accepted February 26, 2017*)

Abstract. Current form of Corrugated-strip connectors are not popular due to the fact that the two ends of this form need to be welded to steel face plates. To overcome this difficulty, a new system is proposed in this work. In this system, bi-directional corrugated-strip connectors are used in pairs, and only one of their ends is welded to the steel face plates on each side. The other end is embedded in the concrete core. To assemble the system, common welding devices are required, and welding process can be performed in the construction sites. By performing the Push-out test under static loading, the authors experimentally assess the effects of geometric parameters on ductility, failure modes and the ultimate shear strength of the aforesaid connectors. For this purpose, sixteen experimental samples are prepared and investigated. For fifteen of these samples, one end of the shear connectors is welded to steel face plates, and the other end is embedded in the concrete. Another experimental sample is prepared in which both ends are welded to the steel face plates. According to the achieved results, several relations are proposed for predicting the ultimate shear strength and load vs. interlayer slip (load-slip) behavior of corrugated-strip connectors. Moreover, these formulas are compared with those of the well-known codes and standards. Accordingly, it is concluded that the authors' relations are more reliable.

Keywords: steel-concrete-steel sandwich; corrugated-strip connectors; push-out test; maximum shear strength; load-slip

1. Introduction

Nowadays, the construction of mega-structures is increased rapidly. This is especially true of engineering structures to be interested in increasing load capacity to structure weight ratios. To achieve this goal, engineers can either find a new structural material or propose a new structural geometry. The first method is time-consuming and expensive. The second one is more applicable because engineers can use any existing composite materials such as a sandwich structure.

For the first time, Solomon *et al*. (1976) proposed steel-concrete-steel (SCS) as a potential structural form to reduce the weight of roadway slab on medium and long span composite bridges. In their study, the precast concrete slab was bonded to steel face plates with the aid of epoxy. Tomlinson *et al*. (1989) developed double skin composite (DSC) or SCS sandwich system with shear studs for immersed tube tunnel application under Conwy River (see Fig. 1-a). In this system one end of studs are welded to the skin, and the other one is embedded in the concrete core.

Since then this material has found further applications for protective structures, building cores, bridge deck, gravity seawalls, floating breakwater, anti-collision structures, nuclear containment, liquid containment, ship hulls and offshore deck structures, in which resistance of impact and explosive loads is of prime importance (Zuk 1974, Oduyemi and Wright 1989, Sohel *et al*. 2003, Bergan and Bakken 2005). Zuk (1974) and Bergan and Bakken (2005) carried out further work to realize its potential for application as lightweight deck structures and for strengthening of weakened areas in ship structures. Valente and Cruz (2010) studied the performance of steel and lightweight concrete composite beams to achieve a good behavior similar to that of normal density concrete. Zou *et al*. (2016) also investigated the influence of interface strength on the failure mode SCS composite beams and failure mechanism leading to final failure of composite beam by experiment and the numerical model to simulate the failure progress.

These extensive applications are due to the fact these materials with different dimensions can be easily constructed in construction sites. Besides, external steel face plates can act as primary reinforcement, permanent formwork and resistant membranes against impact, blast and leakage.

According to available literature review, bottom plate slip, concrete shear failure, possible failure modes of concrete, transverse shear failure and top plate buckling are the main reasons of failure in SCS materials. Besides, in the DSC system when the concrete core is subjected to tensile stresses and cracks, the pull out resistance of the studs maybe gradually lost, especially under cyclic loading (Roberts and Dogan 1998, Dogan and Roberts 2010, 2012). To prevent the occurrence of these failure modes, various shear connectors have been suggested. Bi-steel structure (Bowerman and Chapman 2000) shown in Fig. 1(b)

*Corresponding author, Ph.D., Associate Professor,
E-mail: ghalehnovi@um.ac.ir
[a] Ph.D. Student, E-mail: m_yousefi@cmu.ac.ir

ISSN: 1229-9367 (Print), 1598-6233 (Online)

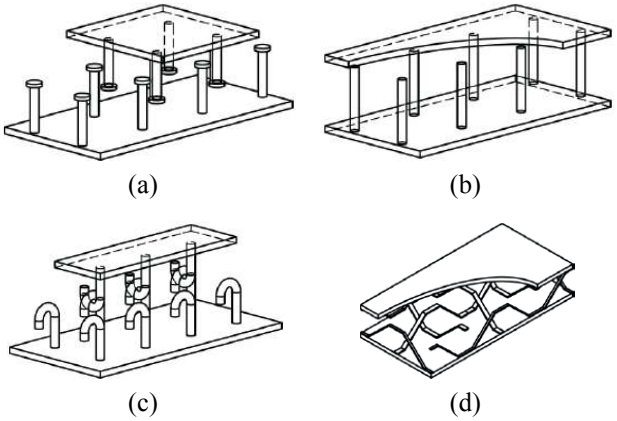

Fig. 1 SCS sandwich constructions based on shear connector shape (a) DSC system; (b) Bi-Steel connectors; (c) J-hook connectors; (d) bi-directional CSC system

performs better than other systems under cyclic loading from the fatigue behavior and local buckling points of view. In this system, both ends of the shear connectors are welded to the steel faces and thus prevented tensile separation and local buckling of face plates. Although Bi-steel sandwich composite plate exhibits excellent structural performances against extreme loads, there is a restriction on minimum core thickness of 200 mm to suit the friction welding equipment.

To resolve this restriction, Liew and Sohel (2009) investigated a new concept for designing composite structures comprising a lightweight concrete core sandwiched in between two steel plates which are interconnected by J-hook connectors (see Fig. 1(c)). The hook connectors are capable of resisting tension and shear forces, and their usage is not restricted by the core thickness. Experimental and numerical studies of SCS sandwich beams, slabs and walls confirms that the J-hook connector is more capable in transferring shear and achieving connection of composite structure between steel plate and concrete core, in comparison to the conventional headed stud connectors (Liew *et al*. 2009, Sohel and Liew 2011, Huang and Liew 2016). Yan *et al*. (2014, 2015) also performed experimental and analytical study on ultimate strength behavior of a variety SCS sandwich beams with ultra-lightweight cement composite (ULCC) and light-weight concrete (LWC).

Investigating SCS structures shows that shear connectors set perpendicular to the steel face plates have been of the most interest to researchers. However, a concrete-filled sandwich beam under bending load suffers from diagonal cracks (Oduyemi and Wright 1989). Hence, Leekitwattana (2011) suggested corrugated-strip connectors (CSC) demonstrated in Fig. 1(d). In contrast to the other shear connectors, these new connectors are placed normal to the diagonal crack line of the concrete. In an analogous manner to Bi-steel system, their ends are welded to the steel face plates. As a consequence, thickness limitation should be considered. Moreover, advanced welding devices are required in this system.

In this work, CSC connectors are employed, and only

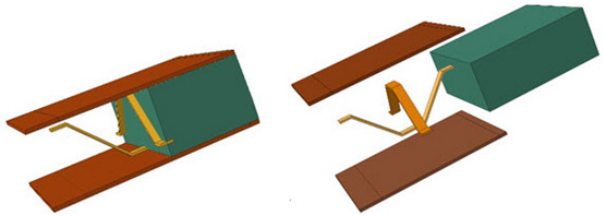

Fig. 2 The modified corrugated-strip connectors in SCS sandwich system

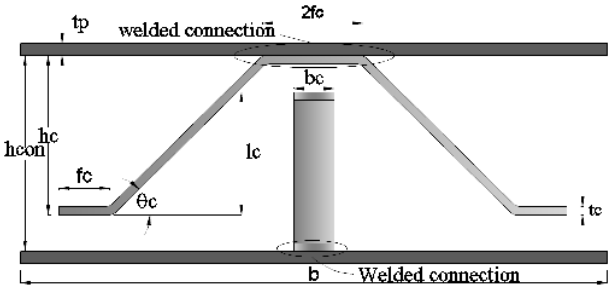

(a) One end welded (DSCS system)

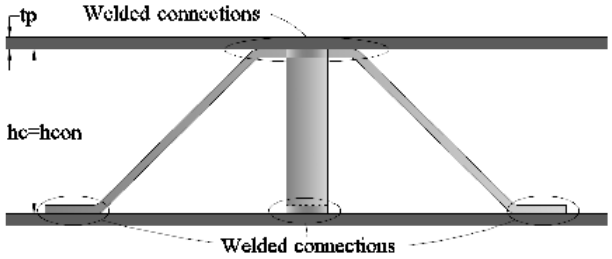

(b) Two end welded (CSC system)

Fig. 3 SCS sandwich system dimensions with corrugated-strip connectors

one of their ends is welded to the steel face plates. The other end is embedded in the concrete core (see Fig. 2). In other words, this modified system is proposed by mixing the DSC and CSC systems, and it is named double skin system with corrugated-strip connectors (DSCS). In this system, common welding devices are required, and welding process can be performed in the construction sites. By providing the sufficient effective welding length, the connectors can be completely connected to the steel face plates. It is expected that the authors' system can resist against interlayer slip under applied loads. Hence, Push-out test is performed on the suggested system. For this purpose, sixteen experimental samples are prepared and investigated. For fifteen of these samples, one end of the shear connectors is welded to the steel face plates, and the other end is embedded in the concrete (see Fig. 3(a)). Another experimental sample is prepared in which both ends are welded to the steel face plates (see Fig. 3(b)). In this way, the effect of various parameters, such as the steel face plates thickness (t_p), the shear connectors width (b_c), the connector sides angle to face plates (θ_c) and the concrete core thickness (h_{con}), connectors overlapped length (l_c), on the behavior of the sandwich system are studied under static loads. It should be mentioned that these parameters are indicated in Fig. 3. Accordingly, several relations are

obtained for predicting the load vs. interlayer slip (load-slip) relationship and shear strength of the authors' system. The accuracy of these formulas is compared with that of the headed stud shear connectors' formulas.

2. Required equipment for performing push-out experiment

By carrying out the Push-out test, the shear strength of two shear connectors can be estimated. This test was firstly performed to evaluate the behavior of Bi-steel shear connectors (Xie *et al*. 2005). Afterwards, other researchers used this test to assess the behavior of other connectors. In this test, a hydraulic jack is needed for loading. Additionally, a load-cell with a capacity of 500 kN and accuracy of 0.01 kN/Sec, a data recorder and processor are required. Moreover, two LVDT should be installed on the upper and lower faces of the concrete core. The load cell transmits the applied load to a block with the thickness of

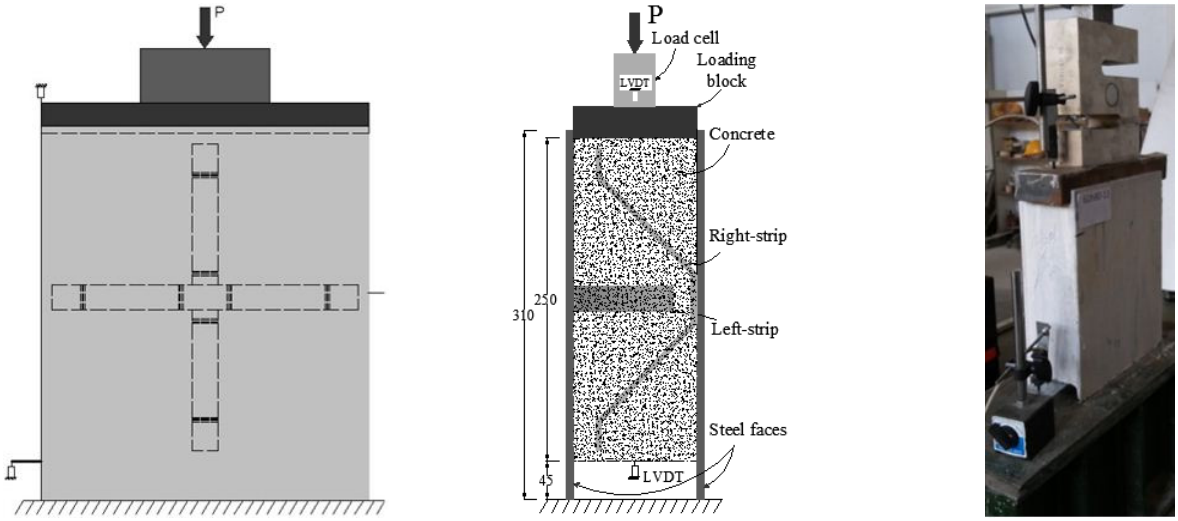

Fig. 4 Test arrangement

Table 1 The geometric dimensions of the DSCS sandwich system

Unit	mm						°	dimensionless		
Specimen	Face plates thickness	Connector width	Flat leg length	Connector height	Connectors overlapped length	Concrete thickness	Connectors sides angle	$hh = h_c/h_{con}$	$lhl = l_c/h_{con}$	$k_{cb} = b_c/b$
	t_p	b_c	f_c	h_c	l_c	h_{con}	θ_c			
6D-1	6	20	27.90	79	56	100	45	0.79	0.56	0.08
8D-2	8	20	27.90	79	56	100	45	0.79	0.56	0.08
10D-3	10	20	27.90	79	56	100	45	0.79	0.56	0.08
12D- 4	12	20	27.90	79	56	100	45	0.79	0.56	0.08
6Db10-5	6	10	27.90	79	56	100	45	0.79	0.56	0.04
6Db70-6	6	70	27.90	79	56	100	45	0.79	0.56	0.28
6Db140-7	6	140	27.90	79	29	127	45	0.62	0.23	0.56
6Db200-8	6	200	27.90	79	0	186	45	0.42	0.00	0.80
6Da90- 9	6	20	25.50	79	56	100	90	0.79	0.56	0.08
6Da60-10	6	20	27.40	79	56	100	60	0.79	0.56	0.08
6Dh100w-11	6	20	26.20	100	100	100	55	1.00	1.00	0.08
6Dh100- 12	6	20	26.20	100	100	100	55	1.00	1.00	0.08
6Dh80- 13	6	20	25.20	79	73	85	53	0.93	0.86	0.08
6Dh65- 14	6	20	25.00	64	58	70	53	0.91	0.83	0.08
6Dh55- 15	6	20	26.00	54	48	60	55	0.90	0.80	0.08
6Dh45- 16	6	20	25.40	44	38	50	54	0.88	0.76	0.08

*Notes: Width of steel face plates b = 250 mm; Thickness of corrugated-strips t_c = 4 mm

(a) Concrete molding

(b) Pouring concrete

Fig. 5 Preparation of sample for Push-out tests

40 mm. this block is placed on the top of the concrete core. In this way, the applied load is uniformly distributed. In Fig. 4, the test arrangement is shown.

3. Experimental process

The geometric parameters of the samples are illustrated in Fig. 3, and their values are listed in Table 1. Recall that; 16 samples are investigated in the Push-out test. The names of the first four samples are in the format of XD-N in which "N" denotes the sample number, and letter "D" stands for DSCS (see Fig. 3(a)). Furthermore, "X" equals to the thickness of the steel face plates. Note that the thickness of the steel face plates of the samples XD-1 to XD-4 are equal to 6 mm, 8 mm, 10 mm and 12 mm, correspondingly. Other samples' thickness of the steel faces is 6 mm. The shear connectors' width of samples 5, 6, 7 and 8 are 10 mm, 70 mm, 140 mm and 200 mm, respectively. Their names are in the format of 6DbY-N in which letter "b" shows that the width of the shear connectors is not constant. The behaviors of these four samples are compared with that of sample 6D-1 in which the width of the shear connectors is 20 mm. The names of the samples 9 and 10 are 6DaY-9 and 6DaY-10, respectively. In this name format, letter "a" denotes the fact that the angle (θ) of corrugate connectors with respect to the steel faces are not constant. Besides, for these samples, "Y" is 60° and 90°, respectively. The behavior of these two samples are compared with that of sample 6D-1. It should be mentioned that θ is 45° in sample 6D-1. The 11th sample's name is 6Dh100w-11 in which "w" shows that the both ends of the shear connectors are welded to the steel faces (see Fig. 3(b)), and h100 shows the thickness of the concrete core is 100 mm. The behavior of this sample is compared with that of sample 6Dh100-12. One end of the 12th sample is welded to the steel face, and the other one is embedded in the concrete. In samples 12 to 16, the core thickness is 100 mm, 85 mm, 70 mm, 60 mm and 50 mm, respectively. In Fig. 5(a), the steel faces placed in concrete molds are illustrated. These molds filled with concrete concrete (see Fig. 5(b)). It should be added that the compre-

Table 2 The mechanical properties of steel

Thickness (mm)	0.2% proof stress (MPa)	Ult. Stress (MPa)	ε_s in Ult. Stress	E_s (GPa)
4	250	380	0.3	207
6	285	495	0.23	202
8	411	615	0.176	205
10	367	620	0.198	203
12	310	516	0.180	207

Table 3 DSCS Push-out test results

Test ref.	P_{exp} (kN)	Failure mode
6D-1	71.16	connectors shear fracture
8D-2	84.51	Left-strip shear fracture & Concrete herringbone shear crack
10D-3	86.7	Top branch bent down & bottom branch straighten of right-strip & concrete wedge shear
12D- 4	82.95	Left-strip shear fracture & Concrete wedge shear
6Db10-5	41.3	Left-strip shear fracture
6Db70-6	114.53	Concrete crushing & plate buckling
6Db140-7	147.62	Concrete wedge splitting
6Db200-8	100	Concrete wedge splitting
6Da90- 9	75.71	Top branch bent down & bottom branch straighten of right-strip & left-strip bent down & concrete crushing
6Da60-10	92.82	Left-strip shear fracture
6Dh100w-11	171.75	Shear connectors fracture & concrete wedge shear
6Dh100- 12	81.36	Connectors shear fracture
6Dh80- 13	86.05	Left-strip shear fracture
6Dh65- 14	72.13	Concrete crushing
6Dh55- 15	75.33	Top branch bent down & bottom branch straighten of right-strip & left-strip bent down & concrete crushing,
6Dh45- 16	68.65	Concrete crushing

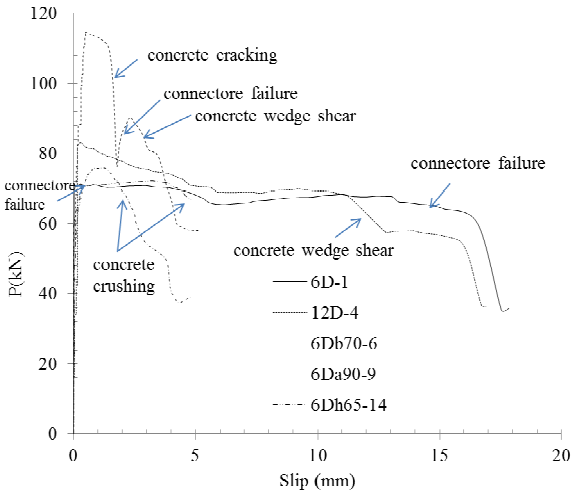

Fig. 6 Illustration on typical static failure modes of the specimens subject to shear force

ssive strength and modulus of elasticity of the used concrete are 37 MPa and 29 GPa, respectively. Tensile test is performed for various thicknesses of the required steel materials and the mechanical properties are listed in Table 2.

4. Push-out test results and discussions

To assess the interlayer slip of steel-concrete-steel composites, Push-out test is performed on the aforesaid samples. The obtained results are presented in the coming sections.

4.1 Failure modes

In Table 3, the maximum recorded load in Push-out test and failure modes under increasing loads are shown. According to Figs. 6 and 7, the failure modes can be investigated. In Fig. 6, the failure modes are specified on the load-

(a) Shear connector fracture

(b) Concrete wedge splitting

(c) Concrete crushing & plate buckling

(d) Right-strip: Top branch bent down & bottom branch straightened

(e) Left-strip bent down

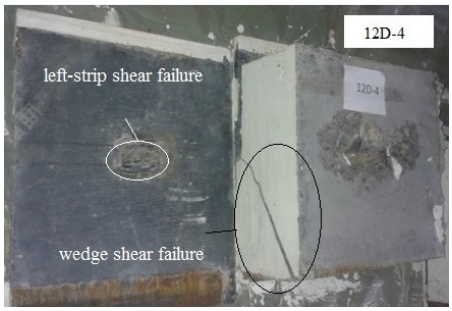

(f) Left-strip shear fracture & concrete wedge shear

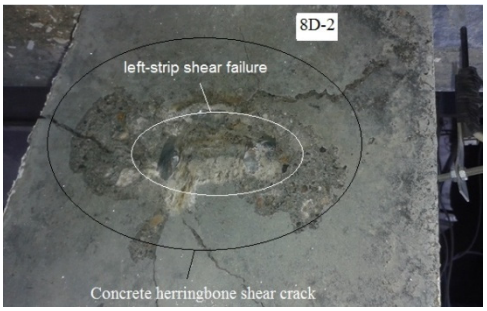

(g) Concrete herringbone shear crack

Fig. 7 Typical static failure modes for the Push-out test of DSCS specimens

slip curves for several experimental samples. In the first part of this curve, the applied load and the slip are linearly dependent. After this linear section, a load-slip relationship is nonlinear. During this test, concrete thickness can prevents from occurrence of concrete splitting. As a result, the shear connectors reach their ultimate loading capacity, and shear connector failure occurs. For sample 6D-1, the aforesaid failure mode is experienced. In addition, deformation of the corrugated-strips of the shear connectors leads to the failure. In this case, top branch of the connectors bend downwards, and the bottom one straightens. As a result, the initial angle of the shear connectors is completely changed. In the samples such as 6Db70-6 in Fig. 7(c) with the steel face plates thickness of 6 mm, plate buckling occurs. The plate buckling can reduce ultimate strength but increase energy absorption. According to Fig. 7(f), in sample 8D-2, the connector branches crush the concrete, and concrete wedge shear occurs in the direction of the right-strip connector. In Figs. 7(g) and (f), samples 8D-2 and 12D-4, the left-strip connector bends down and failure occurs. In this process, concrete herringbone shear crack can be observed. According to Figs. 7(b) and (e), as a result of the concrete thickness reduction and inappropriate angle of shear connectors with respect to the steel faces, the deformation of connectors leads to the concrete wedge shear and concrete crushing, and the ductility is considerably reduced according to Fig. 6. If the concrete core strength is less than the shear connectors strength, concrete cracks. In another words, it behaves in a brittle manner. This failure mode occurs in sample 6Db70-6 in which the connector width is 70 mm. In none of the samples, the welded connections between connectors and steel face plates were failed.

It should be reminded that the steel faces act as a transverse reinforcement, and they can prevent brittle failure of the core. However, in push out test, transverse reinforcement is required for preventing splitting and concrete wedge shear. It should be mentioned that only a pair of shear connector is utilized for DSCS in this work. As a consequence, the core resistance against splitting is weak. This weakness reduces the shear strength of the core. In general, large number of shear connectors is applied in SCS sandwiches. Therefore, the splitting strength of the concrete core increases because of three dimensional stress confinements. In this way, edge connectors connected to the steel faces prevent concrete splitting. Besides, existence of concrete in adjacent cells improves the slip capacity of the shear connectors.

Consequently, the failure of shear connectors can be prevented by using more than two pairs of shear connectors in push out test. This is because of the fact that the upper and lower steel faces require at least two pairs of shear connector to provide splitting strength. In Table 3, the ultimate shear strength and governing failure modes of 16 experimental samples are listed. In what follows, the effect of geometrical parameters on the behavior of the samples is assessed.

4.2 Thickness of the steel plates (t_p)

In Table 3 and Fig. 8, the effect of steel plate thickness on the ultimate shear strength and failure modes of samples 6D-1, 8D-2, 10D-3 and 12D-4 are evaluated. Recall that; the thickness of steel plates in these samples is 6 mm, 8 mm, 10 mm and 12 mm, respectively. In sample 6D-1, the shear connector failure mode occurs, and the steel plates buckle. By increasing the thickness of the plates, they become more rigid. As a consequence, the buckling effects diminish. In this situation, concrete failure mode can be observed in addition to the shear connector failure. The ultimate shear strength of samples 6D-1, 8D-2, 10D-3 and 12D-4 are 71.16 kN, 84.51 kN, 86.7 kN and 82.95 kN, respectively. Consequently, the shear strength converge to a constant value by increasing the thickness. Also, this issue can be observed in Fig. 8(b). According to Fig. 8(a), it is clear that the strength of the aforesaid samples reduces after the reaching the maximum load. Nevertheless, the amount of this reduction in sample 6D-1 is less than other samples. Accordingly, it can be concluded that the load applied to the concrete core is increased by using the more rigid plates, and shear connector failure and concrete fracture modes simultaneously occur.

4.3 Shear connector width to concrete core width ratio

In Table 3 and Fig. 9, the effect of shear connector width (b_c) to concrete core width (b) ratio on the shear strength of samples 6Db10-5, 6D-1, 6Db70-6, 6Db140-7 and 6Db200-8 are assessed. This ratio is denoted by k_{cb}, and it is related to ductility of the samples. It should be reminded that connector width of these samples are 10 mm, 20 mm, 70

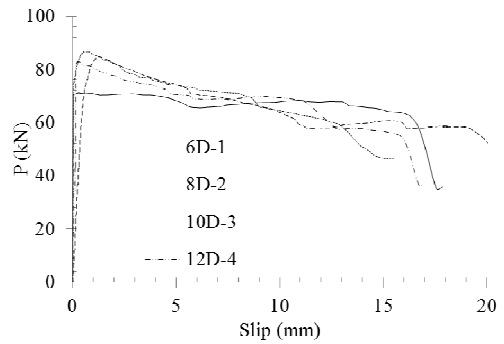

(a) Load-slip curves

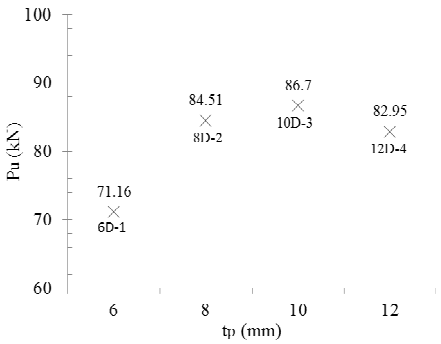

(b) Steel faces thickness (t_p) variations

Fig. 8 The effect of steel faces thickness (t_p) on the load-slip behavior and the ultimate shear strength of DSCS Push-out test

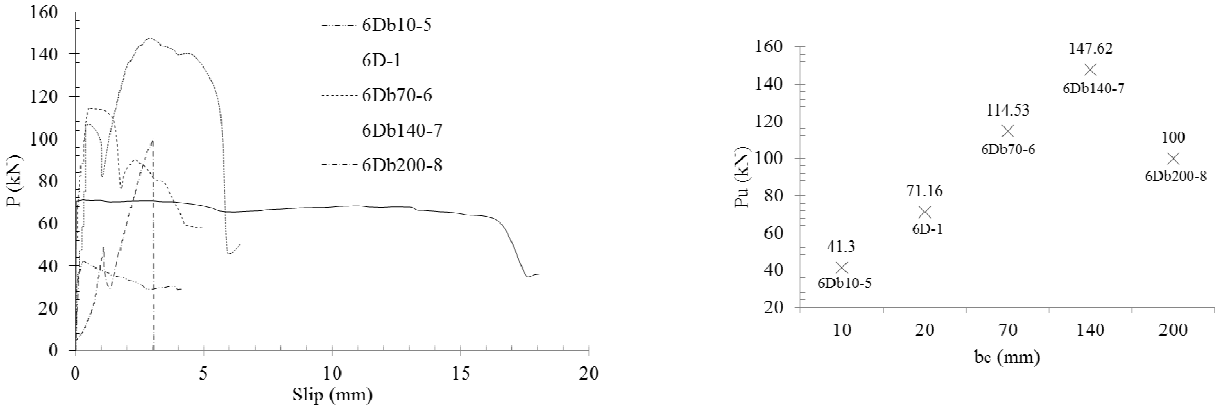

(a) Load-slip curves (b) Width of strip plate (b_c) variations

Fig. 9 The effect of width of strip plate (b_c) on the load-slip behavior and the ultimate shear strength of DSCS Push-out test

mm, 140 mm and 200 mm, respectively. Herein, the width of these samples is 250 mm.

It is worth emphasizing that the ductile behavior is desirable due to the fact that the ultimate capacity of the shear connectors can be applied. In sample 6Db10-5, k_{cb} is 0.04. In this sample, sudden failure of connectors occurs due to the fact that their dimensions are not appropriate. In Sample 6D-1, connectors can reach their ultimate capacity. It should be added that k_{cb} of this sample is 0.08. In sample 6Db70-6, k_{cb} is equal to 0.28. In this sample, concrete core fracture in a brittle manner. In other words, the concrete failure occurs prior to that of the connectors. In samples 6Db140-7 and 6Db200-8, k_{cb} is 0.56 and 0.8, respectively. In these samples, the connector deformation is not sensible, and concrete wedge shear occurs. The ultimate strength of the aforesaid samples are presented in Fig. 9. It is clear that all samples fracture in a brittle manner except for sample 6Db70-6. Accordingly, the brittle fracture of the concrete core occur sooner in samples with greater k_{cb}.

4.4 The angle of connector branches

In this sub-section, samples 6Da90-9, 6Da60-10 and 6D-1 are assessed. The concrete thickness and the connector height of these samples are analogous. The angle of the connector branches are 90°, 60° and 45°, respectively. According to Fig. 10, it is clear that sample 6D-1 is more ductile in comparison to other ones. Based on Fig. 10-b, it is obvious that the ultimate strength of shear connector whose angle is 60° is greater than that of other samples. Clearly, by increasing the angle from 45° to 60°, the ultimate strength of the sample is increased. Moreover, its ductility and energy-absorption is appropriate. In sample 6Da90-9, concrete is crushed and wedge shear occurs because of crack propagation. As a result, the strength is reduced suddenly. Note that concrete failure is prior to connector failure. In general, increasing the angle of 60° to 90° result in reduction of the ductility and strength.

4.5 Two head welding of connectors to steel plates

In this sub-section, the behavior of sample 6Dh100w-11 is compared with sample 6Dh100-12. In sample 6Dh100w-11, two head welding of connectors is used, while one head welding is applied in sample 6Dh100-12. According to Fig. 11, it is clear that the ultimate strength of sample 6Dh100w-11 and 6Dh100-12 are 171.75 kN and 81.36 kN, respectively. In sample 6Dh100w-11, there are four strips that provide face plates connection with both two head welding to faces and by embedding in concrete. While sample 6Dh100-12 includes four strips that provide face plates connection only by embedding in concrete core (see

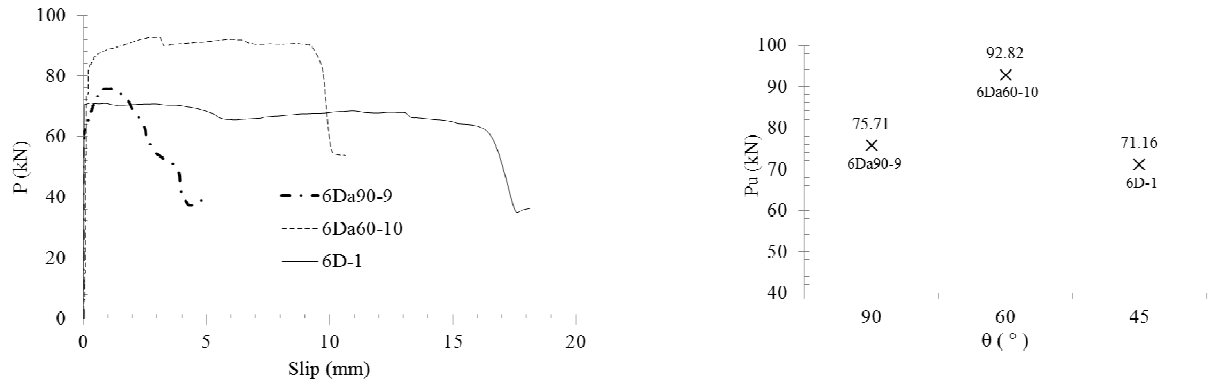

(a) Load-slip curves (b) Parameter θ variations

Fig. 9 The effect of width of strip plate (b_c) on the load-slip behavior and the ultimate shear strength of DSCS Push-out test

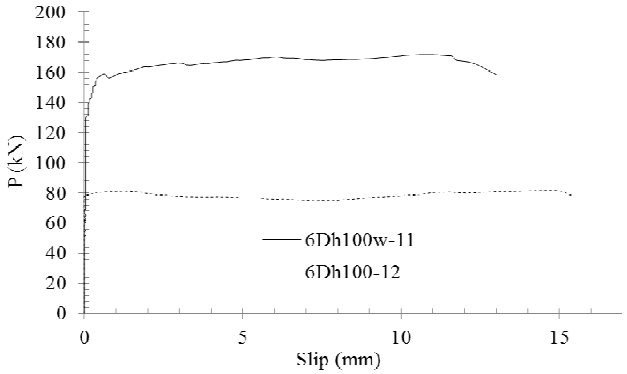

Fig. 11 The effect of one and two head welding connectors on the load-slip behavior and the ultimate shear strength of DSCS Push-out test

Figs. 3(a) and (b)). It should be highlighted that two head welding of corrugated-strip connectors leads to serious problems especially for large dimension structures such as slabs or walls, and thickness limitations are inevitable. However, it requires special facilities in practical operations.

4.6 Concrete core thickness

In this sub-section, samples 6Dh100-12, 6Dh80-13, 6Dh65-14, 6Dh55-15 and 6Dh45-16 are evaluated. The core thickness of these samples is 100 mm, 85 mm, 70 mm, 60 mm and 50 mm, respectively. In these samples, the connector height is 100 mm, 80 mm, 65 mm, 55 mm and 45 mm, respectively. It should be added that $hh = h_c/h_{con}$ is in the range of 0.88 to 1 in these samples. As a result, it is possible to assess the effect of concrete core thickness on the shear strength of DSCSs. According to Table 3 and Fig. 12, it is clear that the ultimate strength of sample 6DH100-12 is 81.36 kN, and shear connector failure occurs for this sample. In sample 6Dh80-13, the shear connectors fail, and the ultimate strength of the sample is 86.05 kN. Obviously, the ultimate strength of this sample is slightly greater than sample 6Dh100-12. This increment is rooted in the volume of concrete and steel used in these samples. In sample 6Dh65-14, the concrete core thickness is 70 mm, and its ultimate strength is 72.13 kN. In comparison to the aforesaid two samples, the connectors deform less, and the concrete is crushed. It is clear that the ultimate strength of samples 6Dh55-15 and 6Dh45-16 are less than that of sample 6Dh100-12, because the concrete core is crushed before reaching the connectors to ultimate strength. Consequently, reducing the concrete thickness decreases the strength of the concrete core, ductility and ultimate strength.

5. Load-slip behavior model

In this section, a behavior model is proposed by using regression method and results obtained from previous sections. This model is required for assessing the load-slip relation and estimating the ultimate strength of the sandwiches structures. For this purpose, researches conducted on headed stud shear connectors are briefly reviewed.

5.1 Behavior model for shear studs

According to experimental results and nonlinear regression analysis, Ollgaard *et al*. (1971) suggested a formula for load-slip model for shear studs

$$\frac{P}{P_u} = (1 - e^{-18\delta})^{0.4} \tag{1}$$

in which the unit of slip (δ) is inch.

An and Cederwall (1996) suggested the next equation for predicting the load response-slip relationship of the shear studs under cyclic loading.

$$\frac{P}{P_u} = \frac{2.24(\delta - 0.058)}{1 + 1.98(\delta - 0.058)} \tag{2}$$

Furthermore, Lorence and Kuica (2006) modified Eq. (1) by performing experimental calibration and proposed the following relation.

$$\frac{P}{P_u} = (1 - e^{0.55\delta})^{0.3} \tag{3}$$

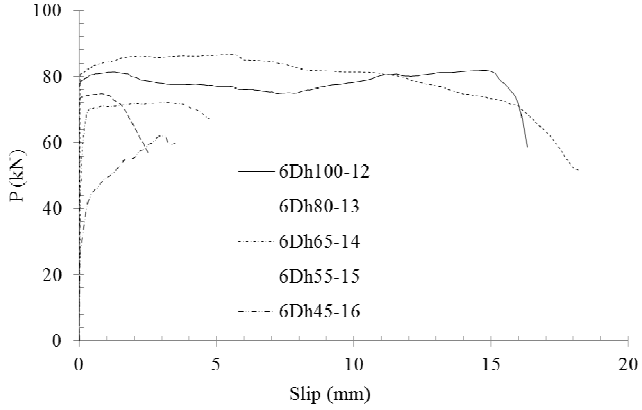

(a) Load-slip curves

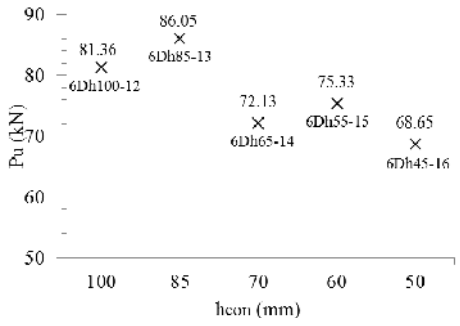

(b) Concrete thickness (h_{con}) variations

Fig. 12 The effect of concrete core thickness (h_{con}) on the load-slip behavior and the ultimate shear strength of DSCS Push-out test

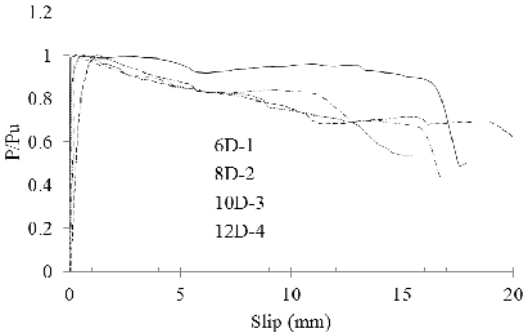

(a) Steel faces thickness variable (t_p)

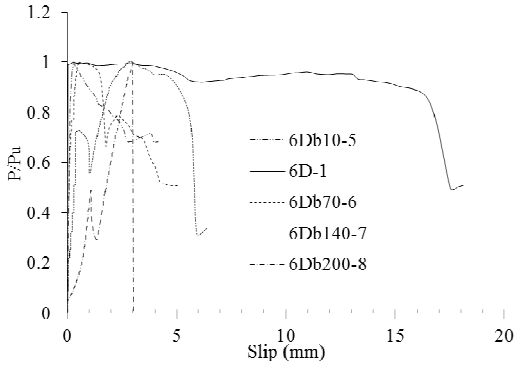

(b) Width of strip plate variable (b_c)

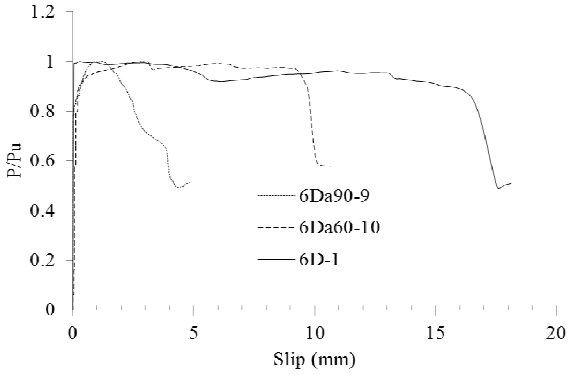

(c) Parameter θ variable

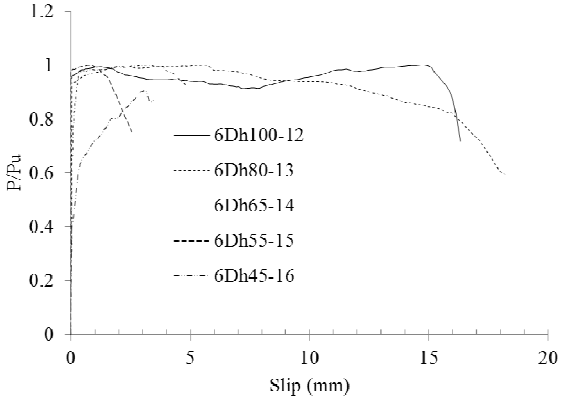

(d) Concrete core thickness variable (h_{con})

Fig. 13 Normalized load-slip curves of DSCS Push-out test

It should be mentioned that slip unit is millimeter in Eqs. (2) and (3).

Besides, Gattesco and Giuriani (1996) proposed the succeeding empirical relation

$$\frac{P}{P_u} = \alpha\sqrt{1 - e^{-\beta\delta/\alpha}} + \gamma\delta \tag{4}$$

where α, β and γ are equal to 0.97 mm^{-1}, 1.3 mm^{-1} and 0.0045 mm^{-1}. These values are obtained by fitting curves to experimental data.

In 2008, Xue *et al*. presented a formula for load-slip model for shear studs, based on the results obtained from performing Push-out test on 30 steel-concrete-steel samples with shear studs. To achieve this goal, they took advantage of works done by Ollgaard *et al*. (1971) and An and Cederwall (1996). This formula has the coming appearance

$$\frac{P}{P_u} = \frac{\delta}{0.5 + 0.97\delta} \tag{5}$$

In this equation, the applied shear load, shear strength of the connector, and slip induced by the applied load are shown by P, P_u and δ, respectively. It should be added that the slip's unit is millimeter in this relation.

5.2 The suggested Load-slip behavior model for DSCS shear connectors

The experimental normalized load (P/P_u) and slip (δ) curves of specimens of DSCS are divided to categories *a*, *b*, *c* and *d*, based on evaluated variables (see Fig. 13). These variables are steel face plates thickness, shear connectors width, angle of the connector branches, and concrete core thickness. To fit correct curve to the data, firstly, samples with sudden strength reduction and concrete wedge shear are omitted. In other words, sample 6Db70-6, 6Db170-7, 6Db200-8, 6Da90-9, 6Dh55-15 and 6Dh45-16 are removed. According to the curves of Fig. 13(a), it is obvious that face plate buckling can be prevented by increasing the thickness of steel faces. As a result, the curves are descending, after ultimate load. This is because of reduction in energy absorption (see Fig. 13(a)). Accordingly, the subsequent relation are presented

$$\frac{P}{P_u} = \frac{100\delta}{1 + 100\delta} - 0.005\delta \qquad (t_p \le 6\,\text{mm}) \tag{6a}$$

$$\frac{P}{P_u} = \frac{100\delta}{1 + 100\delta} - 0.02\delta \qquad (t_p > 6\,\text{mm}) \tag{6b}$$

When the faces buckling are not prevented, Eq. (6a) is used. If the faces buckling are avoided, Eq. (6b) is employed. Based on Fig. 14, these equations can be applied for predicting load response slip relationship in DSCS shear connectors with core made of ordinary concrete. In addition, the angle of the shear connectors should be less than or equal to 60°. Moreover, the brittle fracture of the concrete should be prevented by choosing shear connectors

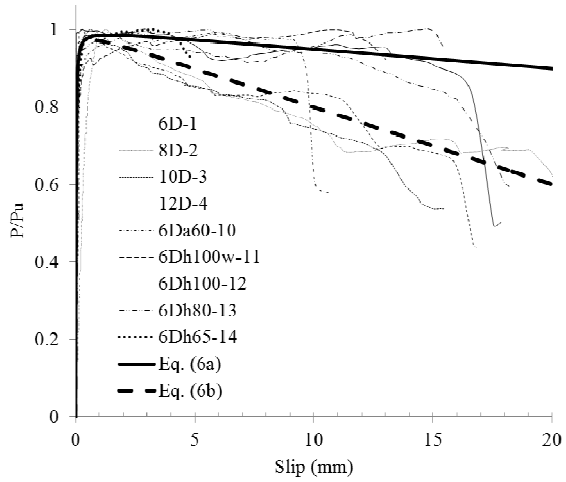

Fig. 14 Comparison between normalized load-slip curves of the test results and the proposed relationships

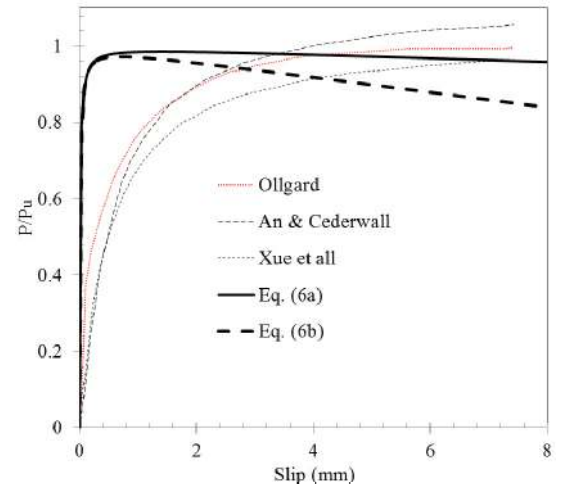

Fig. 15 Comparisons of normalized load-slip curves among different models

with appropriate dimensions.

In Fig. 15, suggested curves for DSCS shear connectors are compared with models proposed for shear studs. In this way, it can be concluded that the stiffness of DSCS connectors are different from that of shear studs. This is because of the differences of geometrical properties of shear connectors.

6. Shear strength of DSCS shear connectors

At this stage, other researchers' formulas for shear strength of headed stud shear connectors are reviewed briefly.

6.1 Available relationships for designing shear studs

Several standards and codes proposed formulas for calculating the shear strength of shear studs. In Eurocode 4 (2004), the shear strength of studs are computed as follows

$$F_u = \min\left(0.8 f_u \frac{\pi d^2}{4\gamma_v}, 0.29\alpha d^2 \sqrt{f_{ck} E_c} / \gamma_v\right) \quad (7)$$

In this relationship, the stud diameter, ultimate tension strength of the stud, cylindrical strength of the concrete, secant elasticity modulus of the concrete and stud height are d, fu, f_{ck}, E_c and h_s, respectively. Moreover, for$3 \le h_s/d < 4$, $\alpha = 0.2(h_s/d + 1)$. For $h_s/d > 4$, $\alpha = 1.0$. Also, γ_v is 1.25. Based on ANSI/AISC 360-10 (2010) , the nominal shear strength of studs embedded in the concrete (used in composite beams with concrete slab) can be calculated by utilizing the next relation

$$F_u = 0.5 A_s \sqrt{f_{ck} E_c} \le 0.75 f_u A_s \quad (8)$$

According to AASHTO Washington (2004), the shear strength of the shear studs embedded in the concrete deck can be computed as below

$$F_u = \phi 0.5 A_s \sqrt{f_{ck} E_c} \le \phi f_u A_s \quad (9)$$

in which ϕ is a strength factor, and it is equal to 0.85. GB 50017-2003 (2003) suggested the succeeding formula for shear strength of studs

$$F_u = 0.43 A_s \sqrt{f_{cp} E_c} \le 0.7\gamma f_u A_s \quad (10)$$

where f_{cp} is the prismatic compressive strength of the concrete, and γ is minimum tension strength of the stud to its yielding stress ratio. Herein it is assumed to be 1.

Eqs. (7)-(10) are developed for studs embedded in the normal weight concrete.

6.2 The suggested formula for shear strength of DSCS' connectors

As previously mentioned, the mechanical properties of all samples are analogous in the current study. The steel face thickness, the angle of shear connector branches, overlap length of the right and left connectors, the length of the inclined branch, stud height to concrete thickness ratio and stud width to concrete width ratio are the main considered parameters. At first, the regression analysis is performed on the aforementioned samples by using statistical software. According to the experimental results, it is concluded that the behavior of sample 6Db200-8 is completely different from other samples. Therefore, it is omitted from regression analysis. The shear strength of the shear connector is dependent variable, and the above-cited parameters are considered as the independent variables. Hence, for samples in which concrete failure modes occur, the shear strength on each side can be written in terms of geometrical parameters as follows

$$\frac{F_u}{A_s} = a\, t_p^b l_c^c h h^d k_{cb}^e \theta_r^f \quad (11)$$

A, b, c, d, e and *f* are coefficients obtained from regression analysis. In this relation, logarithmic transformation is applied. Additionally, for simplicity, a linear formula

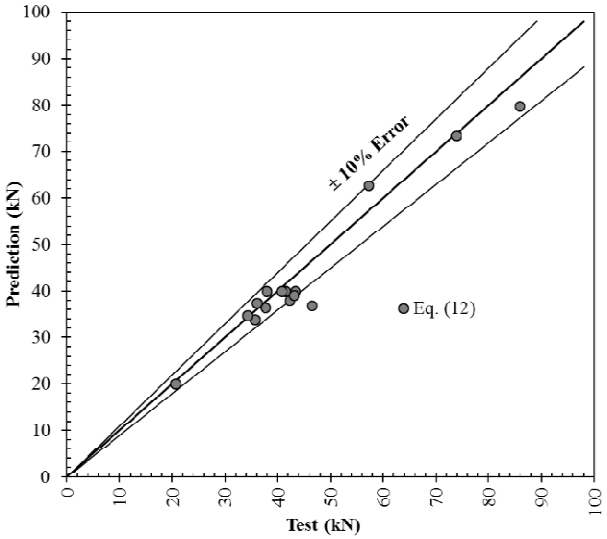

Fig. 16 Comparisons between the test results and predictions by proposed model (Eq. (12))

is developed. It should be mentioned that a linear regression analysis is performed on 15 samples. Recall that, sample 6Db200-8 is omitted for its unusual connector's dimensions. For the cases in which concrete failure modes occur, the following relation is suggested to calculate the shear strength of the DSCS' connectors. It should be mentioned that the least mean squares of this model is equal to 0.1.

$$\frac{F_u}{A_s} = 35.2\, t_p^{0.386} l_c^{0.162} hh^{0.312} k_{cb}^{-0.51} \theta_r^{0.287} \tag{12}$$

6.3 Comparison of the predicted strength with the experimental results

For shear studs, various relations have been presented (Eqs. (7)-(10)). In developing these equations, an equivalent circular cross-section is used instead of the rectangular one for predicting the shear strength of the DSCS' connectors. In Table 4, the shear strength of DSCS' connectors obtained from test is compared with the results achieved from Eqs. (7)-(10) and Eq. (12). In Fig. 16, the dispersion of the experimental results are compared with the predicted ones. Moreover, the authors' relation is compared with those of other researchers for shear studs in Fig. 17. In Fig. 16, the domain whose error is less than or equal to 10% is considered as the safe domain, and the remaining domain is unsafe. Based on the obtained results, increasing k_{cb} from 0.08 to 0.28, 0.56 or 0.8 leads to considerable deviation of the experimental results achieved from the aforementioned relations. This is rooted in the fact that these values of k_{cb} result in concrete fracture prior to the deformation of connectors. This can be observed in samples 6Db140-7 and 6Db200-8. Besides, the overlap length of the connectors is minimum in sample 6Db140-7. It should be added that no overlap length exists in sample 6Db200-8, and it is omitted from investigations.

According to Table 4 and Fig. 17, other researchers' relations are conservative for samples 6Db70-6 and

Table 4 Push-out test results and predictions by different equations

Test ref.	FM*	F_{exp} (kN)	F_{EC4} (kN)	$\frac{F_{exp}}{F_{EC4}}$	F_{AN} (kN)	$\frac{F_{exp}}{F_{AN}}$	F_{AA} (kN)	$\frac{F_{exp}}{F_{AA}}$	F_{GB} (kN)	$\frac{F_{exp}}{F_{GB}}$	F_{prop} (kN)	$\frac{F_{exp}}{F_{prop}}$
1	SC	35.6	39.9	0.89	46.8	0.76	49.9	0.71	43.7	0.81	33.8	1.05
2	CC	42.3	39.9	1.06	46.8	0.90	49.9	0.85	43.7	0.97	37.8	1.11
3	CC	43.3	39.9	1.09	46.8	0.93	49.9	0.87	43.7	0.99	39.9	1.09
4	CC	41.5	39.9	1.04	46.8	0.89	49.9	0.83	43.7	0.95	39.9	1.04
5	SC	20.6	20.0	1.03	23.4	0.88	25.0	0.83	21.8	0.95	20.0	1.03
6	CC	57.3	135.7	0.42	163.8	0.35	174.7	0.33	152.9	0.37	62.5	0.91
7	CC	73.8	211.9	0.35	327.6	0.23	349.4	0.21	305.8	0.24	73.2	1.00
8	---	---	---	--	---	---	---	---	---	---	---	---
9	CC	37.9	39.9	0.95	46.8	0.81	49.9	0.76	43.7	0.87	39.9	0.95
10	SC	46.4	39.9	1.16	46.8	0.99	49.9	0.93	43.7	1.06	36.7	1.26
11	CC	85.9	79.9	1.08	93.6	0.92	99.8	0.86	87.4	0.98	79.9	1.08
12	SC	40.7	39.9	1.02	46.8	0.87	49.9	0.81	43.7	0.93	39.9	1.02
13	SC	43.0	39.9	1.08	46.8	0.92	49.9	0.86	43.7	0.99	38.9	1.10
14	CC	36.1	39.9	0.90	46.8	0.77	49.9	0.72	43.7	0.83	37.3	0.96
15	CC	37.7	39.9	0.94	46.8	0.80	49.9	0.75	43.7	0.86	36.3	1.03
16	CC	34.3	39.9	0.86	46.8	0.73	49.9	0.69	43.7	0.79	34.6	0.99
Ave				**0.92**		**0.78**		**0.73**		**0.84**		**1.04**
Cov				**0.25**		**0.27**		**0.27**		**0.27**		**0.08**

*FM Failure Mode; $F_{exp}= P_{exp}/2$ experimental shear strength of DSCS on each side; F_{EC4} prediction by Eurocode 4; F_{AN} prediction by ANSI/AISC; F_{AA} prediction by AASHTO; F_{GB} prediction by GB50017; F_{Prop} prediction by Eq. (12); CC concrete cracking failure mode; SC shear connector failure mode

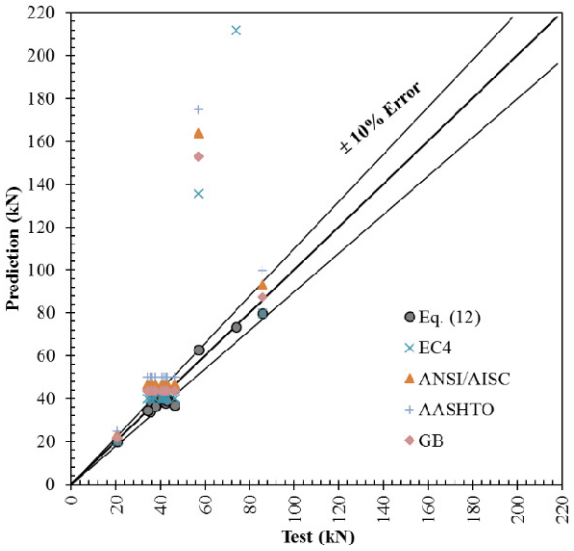

Fig. 17 Comparison between the test results and predictions by different equations

6Db140-7. In what follows, without considering these two samples, the experimental results of other samples are compared with those obtained from these formulas. Based on Table 4, it is obvious that Eq. (7) proposed by Eurocode has the best agreement with the experimental results. The experimental mean to predicted mean ratio is 0.92, and its variance coefficient is 0.25. Based on this relation, 3 samples are placed in the unsafe domain. The mean and variance of the formula presented by GB50017 are 0.84 and 0.27, respectively. 5 samples do not have appropriate fitness. In the safest case, the obtained results are 1.21 times the experimental ones. The results of AASHTO and ANSI/AISC were completely conservative. The proposed formula (Eq. (12)) performs more successfully in comparison to the aforesaid tactics. For this relation, the mean and variance are 1.04 and 0.08. Moreover, all the samples were placed in the safe domain except for samples 8D-2 and 6Da60-10. The error corresponding to the obtained results of samples are 11% and 26%, respectively.

7. Conclusions

In this paper, the load-slip relationship and shear strength of corrugated-strip connectors in composite sandwiches was assessed by performing Push-out test on 16 samples. The obtained results are summarized in what follows.

- In this study, shear failure of the left-strip connectors, flexural failure of the right-strip connectors, buckling of the steel face, concrete wedge shear in the direction of connectors' sides, concrete crushing and concrete herringbone shear crack were observed as failure modes. But, welding failure did not occur in the samples.
- It is concluded that two head welding increase the shear strength of the connectors, twice as many as the one head welding is employed. Additionally, it provides the sufficient ductility. However, serious practical problems are inevitable for two head welding of the corrugated-strip connectors.
- The steel face thickness, overlap length of the connectors, connector height to concrete thickness ratio, the connector width to concrete width ratio and the angle of connector sides with respect to the steel faces are the most important parameters which have effects on the load-slip behavior and shear strength of DSCS. In the authors' relation, these parameters are inserted by introducing exponential coefficients.
- In this work, load-slip curves are defined by $P/P_u = 100\ \delta\ /\ (1 + 100\ \delta) - 0.005\ \delta$ when steel faces buckles. If buckling is prevented, $P/P_u = 100\ \delta\ /\ (1 + 100\ \delta) - 0.02\ \delta$ should be used. Note that, slip unit is mm.

References

AASHTO (2004), Washington DC, USA.

An, L. and Cederwall, K. (1996), "Push-out tests on studs in high strength and normal strength concrete", *J. Constr. Steel Res.*, **36**(1), 15-29.

ANSI/AISC 360-10 (2010), Specification for Structural Steel Buildings; American Institute of Steel Construction, Chicago, IL, USA.

Bergan, P. and Bakken, K. (2005). "Sandwich design: A solution for marine structures", *Proceedings of the International Conference on Computational Methods in Marine Engineering*, *Eccomas Marine*.

Bowerman, H. and Chapman, J. (2000), "Bi-steel concrete steel sandwich construction", *Proceedings of the 4th US Engineering Foundation Conference on Composite Construction*, Banff, Alberta, Canada, May-June.

Dogan, O. and Roberts, T. (2010), "Comparing experimental deformations of steel-concrete-steel sandwich beams with full and partial interaction theories", *Int. J. Phys. Sci.*, **5**(10), 1544-1557.

Dogan, O. and Roberts, T. (2012), "Fatigue performance and stiffness variation of stud connectors in steel–concrete–steel sandwich systems", *J. Constr. Steel Res.*, **70**, 86-92.

Eurocode 4 (2004), Design of Composite Steel and Concrete Structures. Part 1.1: General Rules and Rules for Buildings; BS EN 1994-1-1.

Gattesco, N. and Giuriani, E. (1996), "Experimental study on stud shear connectors subjected to cyclic loading", *J. Constr. Steel Res.*, **38**(1), 1-21.

GB 50017-2003 (2003), Code for design of steel structures; Beijing, China.

Huang, Z. and Liew, J. (2016), "Numerical studies of steel-concrete-steel sandwich walls with J-hook connectors subjected to axial loads", *Steel Compos. Struct., Int. J.*, **21**(3), 461-477.

Leekitwattana, M. (2011), *Analysis of an Alternative Topology for Steel-Concrete-Steel Sandwich Beams incorporating Inclined Shear Connectors*, University of Southampton.

Liew, J.R. and Sohel, K. (2009), "Lightweight steel–concrete–steel sandwich system with J-hook connectors", *Eng. Struct.*, **31**(5), 1166-1178.

Liew, J.R., Sohel, K. and Koh, C. (2009), "Impact tests on steel–concrete–steel sandwich beams with lightweight concrete core", *Eng. Structr,es.* **31**(9), 2045-2059.

Lorenc, W. and Kubica, E. (2006), "Behavior of composite beams prestressed with external tendons: Experimental study", *J. Constr. Steel Res.*, **62**(12), 1353-1366.

Oduyemi, T. and Wright, H. (1989), "An experimental investigation into the behaviour of double-skin sandwich

beams", *J. Constr. Steel Res.*, **14**(3), 197-220.
Ollgaard, J.G., Slutter, R.G. and Fisher, J.W. (1971), "Shear strength of stud connectors in lightweight and normal weight concrete", *AISC Eng. J.*, **8**(2), 55-64.
Roberts, T. and Dogan, O. (1998), "Fatigue of welded stud shear connectors in steel–concrete–steel sandwich beams", *J. Constr. Steel Res.*, **45**(3), 301-320.
Sohel, K. and Liew, J.R. (2011), "Steel–concrete–steel sandwich slabs with lightweight core—Static performance", *Eng. Struct.*, **33**(3), 981-992.
Sohel, K., Richard, L., Alwis, W. and Paramasivam, P. (2003), "Experimental investigation of low-velocity impact characteristics of steel-concrete-steel sandwich beams", *Steel Compos. Struct., Int. J.*, **3**(4), 289-306.
Solomon, S., Smith, D. and Cusens, A. (1976), "Flexural tests of steel-concrete-steel sandwiches", *Magazine of Concrete Research*, **28**(94), 13-20.
Tomlinson, M., Tomlinson, A., Li Chapman, M., Jefferson, A. and Wright, H. (1989), "Shell composite construction for shallow draft immersed tube tunnels", *Immersed Tunnel Techniques: Proceedings of the Conference*, Manchester, UK, April.
Valente, I. and Cruz, P.J. (2010), "Experimental analysis on steel and lightweight concrete composite beams", *Steel Compos. Struct., Int. J.*, **10**(2), 169-185.
Xie, M., Foundoukos, N. and Chapman, J. (2005), "Experimental and numerical investigation on the shear behaviour of friction-welded bar–plate connections embedded in concrete", *J. Constr. Steel Res.*, **61**(5), 625-649.
Xue, W., Ding, M., Wang, H. and Luo, Z. (2008), "Static behavior and theoretical model of stud shear connectors", *J. Bridge Eng.*, **13**(6), 623-634.
Yan, J.-B., Liew, J.R., Zhang, M.-H. and Wang, J. (2014), "Ultimate strength behavior of steel-concrete-steel sandwich beams with ultra-lightweight cement composite, Part 1: Experimental and analytical Study", *Steel Compos. Struct., Int. J.*, **17**(6), 907-927.
Yan, J.-B., Liew, J. and Zhang, M.-H. (2015), "Ultimate strength behavior of steel-concrete-steel sandwich beams with ultra-lightweight cement composite, Part 2: finite element analysis", *Steel Compos. Struct., Int. J.*, **18**(4), 1001-1021.
Zou, G.P., Xia, P.X., Shen, X.H. and Wang, P. (2016), "Investigation on the failure mechanism of steel-concrete steel composite beam", *Steel Compos. Struct., Int. J.*, **20**(6), 1183-1191.
Zuk, W. (1974), "Prefabricated sandwich panels for bridge decks", *Transportation Research Board Special Report*; 148.

CC